original concentration, i.e. 2.5 g dL^{-1} (rHSA), 5.0 g dL^{-1} (DEX), 2.0 g dL^{-1} (MFG), 3.0 g dL^{-1} (HES_{70}), 3.0 g dL^{-1} (HES_{130}), and 3.0 g dL^{-1} (HES_{670}).

Effects of plasma substitutes on the HbV diffusion dynamics in a diluted dispersion. To start with the simplest case, we first tried to investigate variation of the particle diffusion dynamics of the vesicle (without Hb encapsulation) in a diluted suspension in the presence of plasma substitutes and its polymer-concentration dependence. Figure 6 shows the intensity correlation functions, $g_2(t)$, of a diluted vesicle ([lipids] = 0.012 g dL^{-1}) dispersed in various plasma substitute solutions of rHSA, DEX, MFG, HES_{70}, HES_{130}, and HES_{670}, measured at $q = 0.223$ nm^{-1}. The concentrations of these plasma substitutes are varied from 10% to 100% of their original concentrations, while fixing vesicle concentration. Figure 7a shows $g_2(t)$ of the vesicle/rHSA systems. With increasing rHSA concentration, two distinct decays become clearly visible. The faster decay is apparently attributed to the diffusion of rHSAs, and the slower one is to that of the vesicles. Importantly, we observed that $g_2(t)$ at different rHSA concentrations almost simultaneously converges to the baseline at about the same point, demonstrating that a significant slowdown of the vesicle diffusion is not induced by rHSA.

The appearance of two distinct decays is common for all polymers. However, in contrast to the case of rHSA, we found that, as can be seen from Figures 6b-e, all other plasma substitutes cause a pronounced slowdown of the vesicle translational diffusion, and the effect becomes significantly stronger with increasing polymer concentration. In Figure 7, we display the intensity distribution functions $D_I(R_H)$ of vesicle dispersions calculated using ORT[56] from the same DLS data shown in Figure 6a-f, where the data at highest plasma substitute concentrations were chosen. Figure 7 underlines that rHSA does not cause the vesicle flocculation, but other polymers do. In terms of $D_I(R_H)$, the efficacy of the plasma substitutes on the vesicle flocculation are estimated to be in the order of DEX > HES_{670} > MFG > HES_{130} > HES_{70} > rHSA, instead of DEX > MFG> HES_{670} > HES_{70} > HES_{130} > rHSA that is predicted from the depletion potential model. In light of the results, the tendency can broadly be explained with depletion interaction, but there exist some singularity of HES series; (i) the influence of HES_{670} is considerably stronger than expected and (ii) the effect of HES_{130} is stronger than that for HES_{70}, which is opposite to the theoretical prediction. These are likely to be due to unideality of the systems involving the distribution of molecular weights and the complexity of the polymer chain structure.

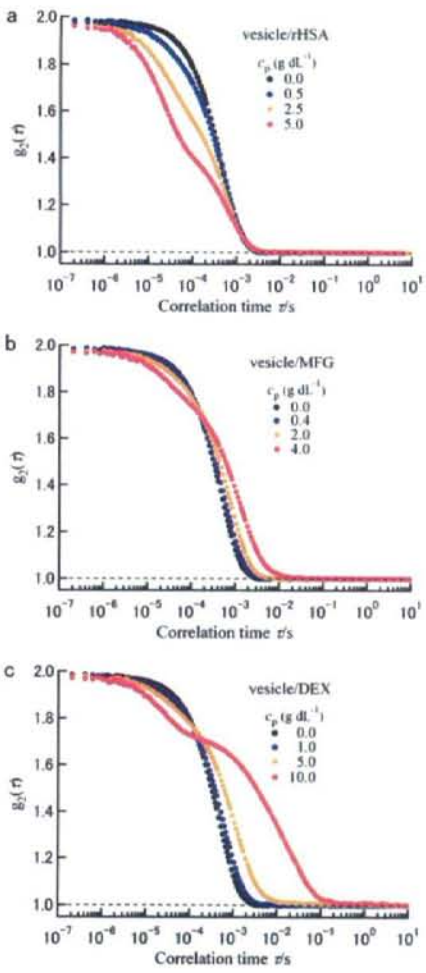

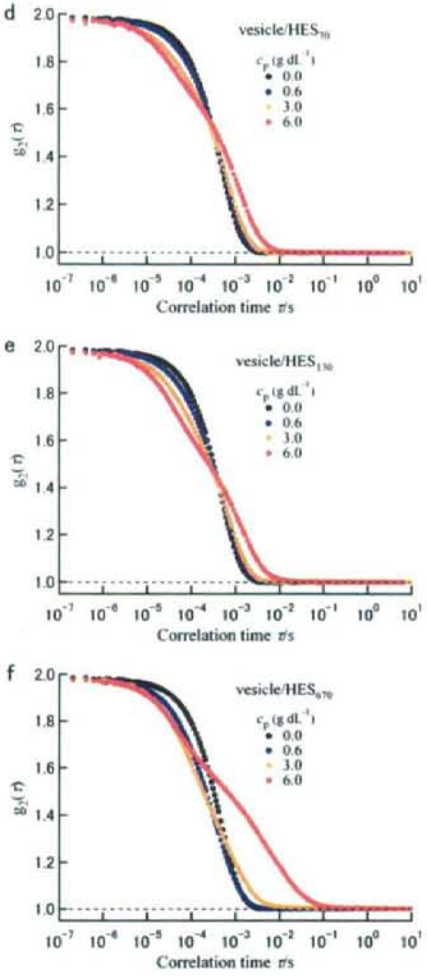

Figure 6: The intensity correlation functions, $g_2(t)$, of a 0.012 g dL^{-1} vesicle suspended in various plasma substitute solutions of rHSA, DEX, MFG, HES_{70}, HES_{130}, and HES_{670}, measured at q = 0.223 nm^{-1}. The concentrations of the plasma substitutes are adjusted to 10%, 50%, and 100% of their original concentration by dilution with saline solution.

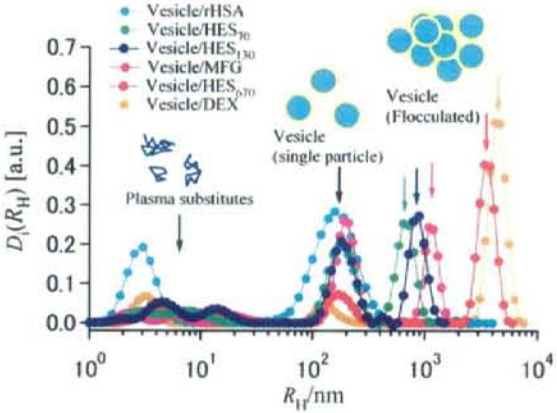

Figure 7: Effect of plasma substitutes on vesicle flocculation in a dilute suspension. The intensity distribution functions, $D_1(R_H)$, of a 0.012 g dL^{-1} vesicle suspended in various plasma substitute solutions of rHSA, DEX, MFG, HES_{70}, HES_{130}, and HES_{670} as a function of hydrodynamic radius, R_H. $D_1(R_H)$ was calculated form the intensity correlation functions, $g_2(t)$, presented in Figure 6 using ORT procedure.[56]

In Figure 8, a partial phase diagram of HbV/polymer mixtures as a function of ϕ_{HbV}, $\eta_p^{(R)}$, and ξ is presented together with a typical theoretical phase diagram of a colloid-polymer mixture (ξ = 0.08),[27] where the reservoir polymer volume fractions $\eta_p^{(R)}$ is estimated for different plasma substitutes at half of their original concentrations; 2.5 g dL^{-1} (rHSA), 5.0 g dL^{-1} (DEX), 2.0 g dL^{-1} (MFG), 3.0 g dL^{-1} (HES_{70}), 3.0 g dL^{-1} (HES_{130}), and 3.0 g dL^{-1} (HES_{670}), using the radius of gyration R_g determined with SAXS data at 1.0 g dL^{-1} (unpublished data). The filled and empty circles represent single liquid and two phases, respectively. In practice, other conditions, e.g., polydispersity and surface charge of the large particle as well as non-ideality of polymer structure especially at high $\eta_p^{(R)}$ may affect the phase behavior. Nevertheless, the figure imply that the phase separation of the HbV suspension in the presence of the

plasma substitutes can be understood based on the depletion interaction potential model for hardsphere mixed with non-adsorbing polymers.

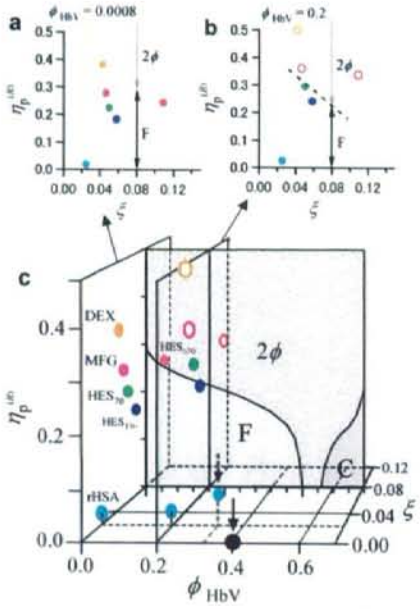

Figure 8: Partial phase diagram of HbV in the presence of plasma substitutes as a function of HbV volume fraction ϕ_{HbV}, reservoir polymer volume fractions $\eta_p^{(R)}$, and the polymer to HbV size ratio ξ, shown together with a theoretical phase diagram of a colloid-polymer mixture ($\xi = 0.08$).[27] Panels **a** and **b** represent 2-D phase diagrams at $\phi_{HbV} = 0.0008$ and $\phi_{HbV} = 0.2$, respectively, and **c** presents a 3-D diagram as a function of ϕ_{HbV}, $\eta_p^{(R)}$, and ξ. F, C, and 2ϕ on the theoretical phase diagram indicate single phase fluid, crystal, and two phase regions, respectively. For $\phi_{HbV} = 0.0008$ and 0.2, the concentration of plasma substitutes was fixed to half of their original ones, i.e., 2.5 g dL^{-1} (rHSA: light blue), 5.0 g dL^{-1} (DEX: orange), 2.0 g dL^{-1} (MFG: pink), 3.0 g dL^{-1} (HES_{70}: right green), 3.0 g dL^{-1} (HES_{130}: blue), and 3.0 g dL^{-1} (HES_{670}: red). Filled and empty circles represent single phase fluid and two-phase, respectively. Arrows highlight the stock HbV dispersion ($\phi_{HbV} = 0.4$) and a currently major applicatory HbV/rHSA mixture ($\phi_{HbV} = 0.32$) used for preclinical tests.

The effects of plasma substitutes on the HbV diffusion dynamics in a dense dispersion. We used TC-DLS to study concentrated HbV/plasma substitute mixtures. In Figures 9a and 9b, we present $g_2(t)$ of the concentrated HbV ([Hb] = 5 g dL^{-1}, [lipids] = 3 g dL^{-1}) and the vesicle without Hb encapsulation ([lipids] = 3 g dL^{-1}) suspended in saline solution and in a series of different plasma substitute solutions of rHSA, HES_{70}, and HES_{130}. In the presence of these plasma substitutes, the decay of $g_2(t)$ becomes apparently slower, indicating the induced depletion forces by plasma substitute (Figures 9a). As shown in Figure 9b, we confirmed that with no reference to Hb-encapsulation, $g_2(t)$ exhibits a similar trend.

In Figure 9c, we compare the TC-DLS result on the concentrated HbV ([Hb] = 8 g dL^{-1}) suspended in 5 g dL^{-1} rHSA solution to that of the dense stock HbV dispersion ([Hb] = 10 g dL^{-1}) in saline solution. We note that rHSA is currently a leading candidate for the co-injected plasma substitute, and most pre-clinical tests of the HbV were carried out using rHSA.[8,9] These two samples exhibit similar single-step behavior of $g_2(t)$ and a rapid decrease to the baseline. This observation provides evidence for ergodicity of these two samples as a nature of single fluid phase, which supports the results obtained in the previous rheological study.

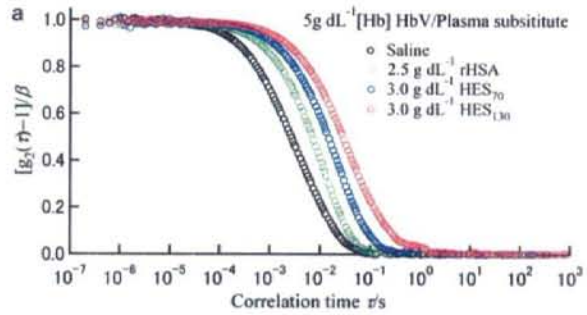

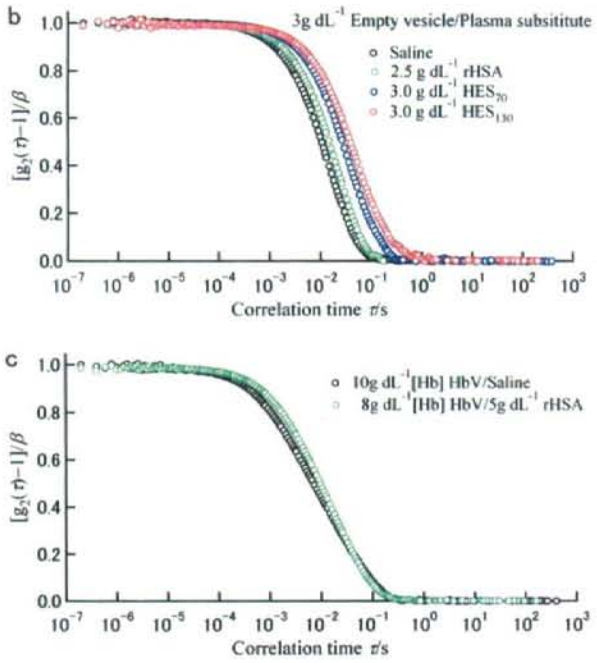

Figure 9: The intensity correlation functions, $g_2(\tau)$, of the concentrated dispersions of HbV and empty uni-lamellar vesicles in saline and plasma substitute solutions; $g_1(\tau)$ of the concentrated HbV dispersions at [Hb] = 1.0, 5.0, and 10 g dL^{-1} (a), the HbV ([Hb] = 5.0 g dL^{-1}) suspended in 2.5 g dL^{-1} rHSA, 3.0 g dL^{-1} HES$_{70}$, and 3.0 g dL^{-1} HES$_{130}$ solutions (b), the 3.0 g dL^{-1} vesicle in the same series of plasma substitutes (c), and the stock HbV dispersion ([Hb] = 10 g dL^{-1}) and the applicatory HbV ([Hb] = 8 g dL^{-1}) in a 5 g dL^{-1} rHSA dispersion in actual medical applications.

Effects of large-molecular-weight HES on the particle motions of HbV. If the HbV is suspended at [Hb] = 5 g dL^{-1} in high concentration solutions of HES$_{670}$, MFG, or DEX, the occurrence of HbV flocculation is apparent. HbV exhibits gradual sedimentation and phase separation, as a red blood cell (RBC) does in normal blood. Note that no hemolysis was observed in these flocculating systems. To

explore the arrested dynamics in the flocculating dispersion, we employed bruteforce[44] and echo DLS[43-45] experiments. The multi-speckle averaging can be achieved in the bruteforce technique by step-by-step altering the sample configurations and performing repeated short time measurements. For a long-time part of ($\tau > 10$ s), the sample cell was precisely rotated to explore many independent sample geometries during one evolution of the rotation to observe echo peaks. The time averaging can essentially be identical with the ensemble averaging.

In Figure 10, we display the field correlation function, $g_1(\tau)$, of the concentrated HbV ([Hb] = 5 g dL^{-1}, [lipids] = 3 g dL^{-1}) dispersed in a series of 3 g dL^{-1} HES solutions. The data of HbV/HES$_{670}$ dispersion were measured with the brute-force and echo DLS techniques in the TC configuration, and other $g_1(\tau)$ functions for HbV in saline and in the lower-molecular-weight HES solutions (HES$_{130}$ and HES$_{70}$) are converted from the same $g_2(\tau)$ data already shown in Figure 9a. In contrast to the rapid single-step relaxation behavior and apparently ergodic nature of the HbV/saline, HbV/HES$_{70}$, and HbV/HES$_{130}$ systems, the HbV/HES$_{670}$ dispersion shows a significant slowdown of the particle diffusion dynamics and looks like nonergodic within our time window (up to 3×10^4 sec). The process is characterized by the two-step behavior of $g_1(t)$, showing a faster decay with a small amplitude of ca. 0.15, and the following second slower decay. This observation demonstrates that the short-range particle diffusion is highly restricted in a flocculating system due to the depletion (polymer-induced adhesive) interaction between the HbV particles. The slower decay appears to reflect the slow dynamics of the large HbV flocculation in a HbV rich-phase of the phase separated dispersion, which certainly involves an aging effect during the echo experiment. Although we did not perform echo measurements for the HbV/DEX and HbV/MFG dispersions, repeated short-time DLS measurements with rotating the sample cell gave strong fluctuations of the intercept (coherence factor). This is a clear signature of the non-ergodicity or gradual phase-separation of these samples.

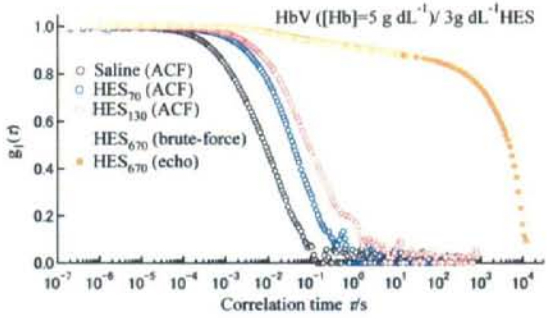

Figure 10: The field correlation functions, $g_1(t)$, of the concentrated HbV ([Hb] = 5 g dL^{-1}, [Lipids] = 3 g dL^{-1}) dispersed in saline and in a series of HES solutions. The $g_1(t)$ of the HbV/HES$_{670}$ was measured using bruteforce and echo DLS techniques in the thin layer cell configuration. The $g_1(t)$ data on the HbV in saline and in the lower-molecular-weight HES solutions (HES$_{70}$ and HES$_{130}$) were converted from the $g_2(t)$ data shown in Figure 9a.

Conclusions

We have investigated static structure and dynamics of HbV, a cellular-type artificial oxygen carrier functionalized as a transfusion alternative. DLS data on a diluted HbV dispersion evaluated by optimized regularization technique (ORT) yielded an averaged hydrodynamic diameter of 238 nm and a 20 nm standard deviation in volume distribution. The SAXS data on the vesicle for Hb encapsulation confirmed its uni-lamellar structure as designed, and the IFT analysis provided the thickness (ca. 5.8 nm) and internal electron density profiles of the bilayer membrane. Consistent with the DLS data, the forward SAXS intensity of the HbV dispersion exhibits a feature of polydisperse spherical particles having an averaged radius of ca 120 nm, while its high q-part manifests the internal density fluctuations

static structure factor of the encapsulated Hbs are quite similar to those in bulk Hb solution at identical protein concentration. The finding demonstrates that confinement into an inner aqueous phase of the vesicle (ca. 240 nm ϕ) does not significantly affect the interparticle interaction of Hbs. TC-DLS combined with the bruteforce and echo technique enables us to overcome the interference from multiple scattering of a turbid sample and thus makes it possible to observe collective diffusion of a concentrated HbV dispersion in the presence of various plasma substitutes (water-soluble polymers used to maintain colloid osmotic pressure of blood in medical treatments) without dilution. It should also be mentioned that this technique is perfectly non-invasive, i.e. no external force is applied to the system like in rheology. During the duration of these experiments, the HbV dispersions were perfectly stable. Actually, we confirmed that the dispersion stability of HbV and the oxygen binding function of encapsulated HbV were preserved for over two years at room temperature.[48] In contrast to the rapid single-step relaxation behavior and apparently ergodic nature of the HbV/saline, HbV/HES$_{70}$, and HbV/HES$_{130}$ systems, the HbV/HES$_{670}$ dispersion shows two-step behavior of $g_1(t)$, which looks like nonergodic within our time window; a faster decay with a small amplitude and the following second slower decay indicate that the short-range particle diffusion is strongly restricted in a flocculating system due to the depletion interaction between the HbV particles, while the slow mode appears to reflect the slow dynamics of the

HbV flocculation in a HbV rich-phase of the phase separated dispersion. We note that as we confirmed in the previous rheological study,[32] such a HbV flocculation dissociates rapidly under a shear flow and is completely reversible.

Despite a controversy on the mechanism of liposome flocculation, our DLS results, simulated structure factor, and the phase behavior, demonstrate that the underlying mechanism of the HbV flocculation in the presence of plasma substitutes is due to depletion interaction; exclusion of polymer molecules from the region closely spaced HbV particles induces an effective attractive potential between the HbVs, increasing the overall disorder of the system. At the same time, a pending question about a significantly weaker effect of rHSA on HbV flocculation and suspension viscosity enhancement than those induced by other polymers is clearly answered. This is attributed to a compact native structure of the protein, which efficiently reduces the reservoir polymer volume fraction, and thus suppresses the strength of the depletion forces. The significance of these entropically driven phenomena is highlighted by the tunable suspension rheology of HbVs using different combination of plasma substitute solutions. High viscosity fluid is occasionally advantageous for sustaining peripheral blood flow, giving shear stress on the vascular wall to facilitate the production of vasorelaxation factors. The results are not only implicative in the fields of soft-condensed matter physics and bio-chemistry, but of interdisciplinary importance for a new class of forthcoming medical applications.

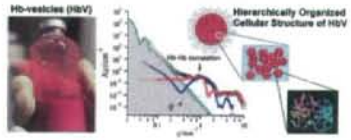

Acknowledgement The authors thank Dr. Dominique Erni (Inselspital Hospital, Univ. of Berne), Dr. Amy G. Tsai (Univ. of San Diego), Dr. Masahiko Takaori (East Takarazuka Sato Hospital), and Dr. Koichi Kobayashi (Keio Univ.) for their cooperation and meaningful discussions. This work was supported in part by Health Sciences Research Grants (Research on Publicly Essential Drugs and Medical Devices, H18-Soyaku-Ippan-022), from the Ministry of Health, Labour and Welfare, Japan (H.S., E.T.), Grants-in-Aid for Scientific Research from Japan Society for the Promotion of Science (B19300164) (H.S.), and Young Researchers Empowerment Project of Shinshu University (T.S.) from the Ministry of Education, Culture, Sports, Science and Technology (MEXT), Japan. M.M. and O.G. acknowledge financial support by the European Marie-Curie Research and Training Network on Arrested Matter under Grant No. MRTN-CT-2003-504712. The rHSA, HES$_{130}$, and MFG used in this study were gifts respectively from Nipro Co., Fresenius Kabi A.G., and B. Braun.

References

(1) Torchilin, V. P. *Nat. ReV. Drug DiscoVery* **2005**, *4*, 145-160

(2) Izumi, Y.; Sakai, H.; Hamada, K.; Takeoka, S.; Yamahata, T.; Kato, R.; Nishide, H.; Tsuchida, E.; Kobayashi, K. *Crit. Care Med.* **1996**, *24*, 1869-1873.

(3) Sakai, H.; Takeoka, S.; Park, S. I.; Kose, T.; Nishide, H.; Izumi, Y.; Yoshizu, A.; Kobayashi, K.; Tsuchida, E. *Bioconjugate Chem.* **1997**, *8*, 23-30.

(4) Chang, T. M. *Artif. Organs* **2004**, *28*, 789-794.

(5) Djordjevich, L.; Miller, I. F. *Exp. Hematol.* **1980**, *8*, 584-592.

(6) Phillips, W. T.; Klipper, R. W.; Awasthi, V. D.; Rudolph, A. S.; Cliff, R.; Kwasiborski, V.; Goins, B. A. *J. Pharmacol. Exp. Ther.* **1999**, *288*, 665-670.

(7) Sakai, H.; Horinouchi, H.; Yamamoto, M.; Ikeda, E.; Takeoka, S.; Takaori, M.; Tsuchida, E.; Kobayashi, K. *Transfusion* **2006**, *46*, 339-347.

(8) Sakai, H.; Masada, Y.; Horinouchi, H.; Yamamoto, M.; Ikeda, E.; Takeoka, S.; Kobayashi, K.;

(9) Yamazaki, M.; Aeba, R.; Yozu, R.; Kobayashi, K. *Circulation* **2006**, *114*, I220-I225.

(10) Sakai, H..; Sou, K.; Horinouchi, H.; Kobayashi, K.; Tsuchida, E. *J. Intern. Med.* **2008**, *263*, 4-15.

(11) Liu X.; Miller, M. J.; Joshi, M. S.; Sadowaska-Krowicka, H.; Clark, D. A.; Lancaster, J. R. Jr. *J. Biol. Chem.* **1998**, *273*, 18709-19713.

(12) Vaughn, M. W.; Huang, K. T.; Kuo, L.; Liao, J. C. *J. Biol. Chem.* **2000**, *275*, 2342-2348.

(13) Sakai, H.; Sato, A.; Takeoka, S.; Tsuchida, E. *J. Biol. Chem.* **2008**, *283*, 1508-1517.

(14) Sakai, H.; Hara, H.; Yuasa, M.; Tsai, A.G.; Takeoka, S.; Tsuchida, E.; Intaglietta, M. *Am. J. Physiol. Heart Circ. Physiol.* **2000**, *279*, H908-H915.

(15) Takeoka, S.; Ohgushi, T.; Terase, K.; Ohmori, T.; Tsuchida, E. *Langmuir* **1996**, *12*, 1755-1759.;

(16) Takeoka, S.; Terase, K.; Sakai, H.; Yokohama, H.; Nishide, H.; Tsuchida, E. *J. Macromol. Sci., Pure Appl. Chem.* **1994**, *A31*, 97-108.

(17) Glatter, O.; Kratky, O. *Small-Angle X-ray Scattering;* Academic: London, **1982**.

(18) Lindner, P.; Zemb, Th. Eds.; *Neutron, X-Ray and Light Scattering:* North-Holland: Amsterdam, **1991**.

(19) Peters, T. All About Albumin: Biochemistry, Genetics, and Medical Applications (Academic, New York, 1996).

(20) Meyuhas, D.; Nir, S.; Lichtenberg, D. *Biophys. J.* **1996**, *71*, 2602-2612.

(21) Sunamoto, J.; Iwamoto, K.; Kondo, H. *Biochem. Biophys. Res. Commun.* **1980**, *94*, 1367-1373.

(22) Otsubo, Y. *Langmuir* **1990**, *6*, 114-118.

(23) Tilcock, C. P.; Fisher, D. *Biochim. Biophys. Acta* **1982**, *688*, 645-652.

(24) Neu, B.; Meiselman, H. J. *Biophys. J.* **2002**, *83*, 2482-2490.

(25) Goto, Y.; Sakakura, S.; Hatta, M.; Sugiura, Y.; Kato, T. *Acta Anaesthesiol. Scand.* **1985**, *29*, 217-223.

(26) Asakura, S.; Oosawa, F. *J. Chem. Phys.* **1954**, *22*, 1255-1256.

(27) [illegible]

(28) Vrij, A. *Pure Appl. Chem.* **1976**, *48*, 471-483.

(29) Bergenholtz, J.; Poon, W. C. K.; Fuchs, M. *Langmuir* **2003**, *19*, 4493-4503.

(30) Lekkerkerker, H. N. W.; Poon, W. C. K.; Pusey, P. N.; Stroobants, A.; Warren, P.B. *Europhys. Lett.* **1992**, *20*, 559-564.

(31) Ilett, S.M.; Orrock, A.; Poon, W. C. K.; Pusey, P. N. *Phys.Rev. E* **1995**, *51*, 1344-1352.

(32) Sakai, H.; Sato, A.; Takeoka, S.; Tsuchida, E. *Langmuir* **2007**, *23*, 8121-8128.

(33) Contaldo, C.; Plock, J.; Sakai, H.; Takeoka, S.; Tsuchida, E.; Leunig, M.; Banic, A; Erni, D. *Crit. Care Med.* **2005**, *33*, 806-812.

(34) Tsai, A. G.; Acero, C.; Nance, P. R.; Cabrales, P.; Frangos, J. A.; Buerk, D. G.; Intaglietta, M. *Am. J. Physiol. Heart Circ. Physiol.* **2005**, *288*, H1730-H1739.

(35) Tsai, A. G.; Intaglietta, M. *Biorheology* **2001**, *38*, 229-237.

(36) de Wit, C.; Schafer, C.; von Bismarck, P.; Bolz, S. S.; Pohl, U. *PflugersArch.* **1997**, *434*, 354-361.

(37) Kobayashi, K. *Biologicals* **2006**, *34*, 55-59.

(38) Sakai, H.; Tsai, A. G.; Kerger, H.; Park, S. I.; Takeoka, S.; Nishide, H.; Tsuchida, E.; Intaglietta, M. *J. Biomed. Mater. Res.* **1998**, *40*, 66-78.

(39) Webb, A. R.; Nash, G. B.; Dormandy, J. A.; Bennett, E. D. *Clin. Hemorheol.* **1990**, *10*, 287-296.

(40) Webb, A. R.; Barclay, S. A.; Bennett, E. D. *IntensiVe Care Med.* **1989**, *15*, 116-120.

(41) Traylor, R. J.; Pearl, R. G. *Anesth. Analg.* **1996**, *83*, 209-212.

(42) Medebach, M.; Moitzi, C.; Freiberger, N.; Glatter, O. *J. Colloid int. Sci.* **2007**, *305*, 88-93.

(43) Medebach, M.; Freiberger, N.; Glatter, O. *Rev. Sci. Instrum.* **2008**, *79*, 073907 (1-12).

(44) Pham, K. N.; Egelhaaf, S. U.; Pusey, P. N.; Poon, W. C. K.; *Phys. Rev. E* **2004**, *69*, 011503-1-13.

(45) Pham, K. N.; Egelhaaf, S. U.; Moussaïd, A.; Pusey, P. N. *Rev. Sci. Instrum.* **2004**, *75*, 2419-2431.

(46) Sou, K.; Naito, Y.; Endo, T.; Takeoka, S.; Tsuchida, E. *Biotechnol. Prog.* **2003**, *19*, 1547-1552.

(47) Sakai, H.; Masada, Y.; Takeoka, S.; Tsuchida, E. *J. Biochem. (Tokyo)* **2002**, *131*, 611-617.

(48) Sakai, H.; Tomiyama, K.; Sou, K.; Takeoka, S.; Tsuchida, E. *Bioconjugate Chem.* **2000**, *11*, 425-432.

(49) Orthaber, D., Bergmann, A. and Glatter, O. *J. Appl. Crystallogr.* **2000**, *33*, 218-225.

(50) Schnablegger, H.; Glatter, O. *Appl. Opt.* **1995**, *34*, 3489-3501.

(51) Lehner, D.; Kellner, G.; Schnablegger, H.; Glatter, O. *J. Colloid Int. Sci.* **1998**, *201*, 34-47.

(52) Weyerich, B.; Brunner-Popela, J.; Glatter, O. *J. Appl. Crystallogr.* **1999**, *32*, 197-209.

(53) Fritz, G.; Bergmann, A.; Glatter, O.; *J. Chem. Phys.* **2000**, *113*, 9733-9740.

(54) Fritz, G.; Glatter, O. *J. Phys.: Condens. Matter* **2006**, *18*, S2403-S2419.

(55) Koppel, D. E. *J. Chem. Phys.* **1972**, *57*, 4814-4820.

(56) Schnablegger, H.; Glatter, O. *Appl. Opt.* **1991**, *30*, 4889-4896.

(57) Frühwirth, T.; Fritz, G.; Freiberger, N.; Glatter, O. *J. Appl. Cryst.* **2004**, *37*, 703-710

(58) Glatter, O. *J. Appl. Cryst.* **1980**, *13*, 577-584.

(59) Glatter, O. *J. Appl. Cryst.* **1977**, *10*, 415-421.

(60) Sou, K.; Endo, T.; Takeoka, S.; Tsuchida, E. *Bioconjugate Chem.* **2000**, *11*, 372-379.

(61) Sato, T.; Sakai, H.; Sou, K.; Buchner, R.; Tsuchida, E. *J. Phys. Chem. B* **2007**, *111*, 1393-1401.

(62) Glatter, O. *J. Appl. Cryst.* **1981**, *14*, 101-108.

(63) Glatter, O. *Prog. Colloid Polym. Sci.* **1991**, *84*, 46-54.

(64) Mittelbach, R.; Glatter, O. *J. Appl. Cryst.* **1998**, *31*, 600-608.

(65) Rodriguez, C.; Naito, N.; Kunieda, H. *Colloid Surf. A* **2001**, *237*-246, 181.

(66) Sato, T.; Komatsu, T.; Nakagawa, A.; Tsuchida.E. *Phys. Rev. Lett.* **2007**, *98*, 208101 (1-4).

(67) Stradner, A.; Sedgwick, H.; Cardinaux, F.; Poon, W. C. K.; Egelhaaf, S. U.; Schurtenberger, P. *Nature* **2004**, *432*, 492-495.

(68) Liu, Y.; Chen, Fratini, E.; Baglioni, P.; W. R.; Chen, S. H. *Phys. Rev. Lett.*, **2005**, *95*, 118102 (1-4).

(69) Stradner, A.; Thurston, G. M.; Schurtenberger, P. *J. Phys.: Condens. Matter* **2005**, *17*, S2805–S2816.

(70) Chihara, J.; *Prog. Theor. Phys.* **1973**, *50*, 409-423.

(71) Madden W. G.; Rice, S. A. *J. Chem. Phys.* **1980**, *72*, 4208-4215.

平成20年度厚生労働省科学研究費補助金
政策創薬総合研究推進事業　研究成果等普及啓発事業

平成20年度 研究成果発表会

人工血液をつくる(9)

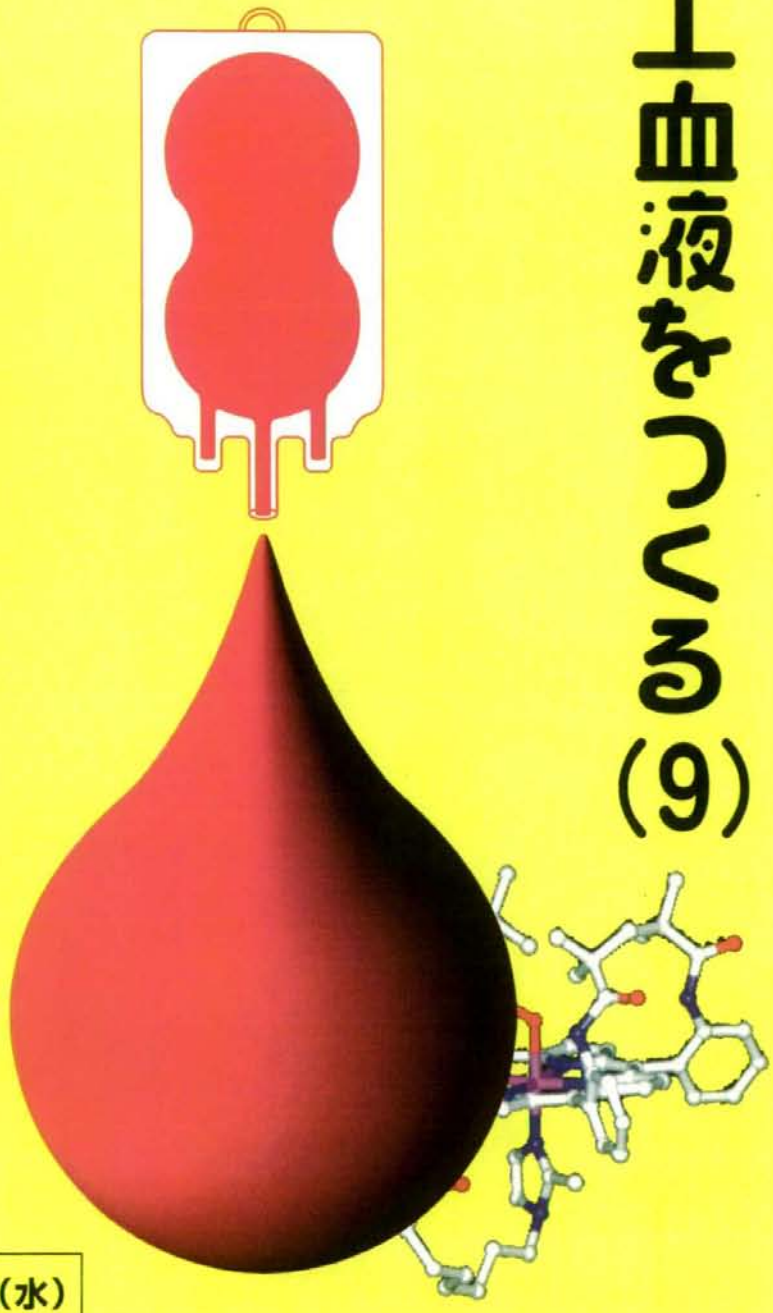

平成21年2月11日(水)
時間:9:00～17:10
慶應義塾大学信濃町キャンパス
医学情報センター　北里講堂
定員:250名

主　催：財団法人　ヒューマンサイエンス振興財団
後　援：日本血液代替物学会